Am J Physiol Lung Cell Mol Physiol 303: L939–L952, 2012.
First published September 21, 2012; doi:10.1152/ajplung.00034.2012.

CALL FOR PAPERS | *Bioengineering the Lung: Molecules, Materials, Matrix, Morphology, and Mechanics*

Rho-kinase inhibition attenuates airway responsiveness, inflammation, matrix remodeling, and oxidative stress activation induced by chronic inflammation

Samantha Souza Possa,[1] Homar Toledo Charafeddine,[1] Renato Fraga Righetti,[1] Patricia Angeli da Silva,[1] Rafael Almeida-Reis,[1] Beatriz Mangueira Saraiva-Romanholo,[1] Adenir Perini,[1] Carla Máximo Prado,[2] Edna Aparecida Leick-Maldonado,[1] Milton A. Martins,[1] and Iolanda de Fátima Lopes Calvo Tibério[1]

[1]*Department of Medicine, School of Medicine, University of São Paulo, and* [2]*Department of Biological Science, Federal University of São Paulo, Diadema, São Paulo, Brazil*

Submitted 30 January 2012; accepted in final form 19 September 2012

Possa SS, Charafeddine HT, Righetti RF, da Silva PA, Almeida-Reis R, Saraiva-Romanholo BM, Perini A, Prado CM, Leick-Maldonado EA, Martins MA, Tibério ID. Rho-kinase inhibition attenuates airway responsiveness, inflammation, matrix remodeling, and oxidative stress activation induced by chronic inflammation. *Am J Physiol Lung Cell Mol Physiol* 303: L939–L952, 2012. First published September 21, 2012; doi:10.1152/ajplung.00034.2012.—Several studies have demonstrated the importance of Rho-kinase in the modulation of smooth muscle contraction, airway hyperresponsiveness, and inflammation. However, the effects of repeated treatment with a specific inhibitor of this pathway have not been previously investigated. We evaluated the effects of repeated treatment with Y-27632, a highly selective Rho-kinase inhibitor, on airway hyperresponsiveness, oxidative stress activation, extracellular matrix remodeling, eosinophilic inflammation, and cytokine expression in an animal model of chronic airway inflammation. Guinea pigs were subjected to seven ovalbumin or saline exposures. The treatment with Y-27632 (1 mM) started at the fifth inhalation. Seventy-two hours after the seventh inhalation, the animals′ pulmonary mechanics were evaluated, and exhaled nitric oxide (E_{NO}) was collected. The lungs were removed, and histological analysis was performed using morphometry. Treatment with Y-27632 in sensitized animals reduced E_{NO} concentrations, maximal responses of resistance, elastance of the respiratory system, eosinophil counts, collagen and elastic fiber contents, the numbers of cells positive for IL-2, IL-4, IL-5, IL-13, inducible nitric oxide synthase, matrix metalloproteinase-9, tissue inhibitor of metalloproteinase-1, transforming growth factor-β, NF-κB, IFN-γ, and 8-iso-prostaglandin F2α contents compared with the untreated group ($P < 0.05$). We observed positive correlations among the functional responses and inflammation, remodeling, and oxidative stress pathway activation markers evaluated. In conclusion, Rho-kinase pathway activation contributes to the potentiation of the hyperresponsiveness, inflammation, the extracellular matrix remodeling process, and oxidative stress activation. These results suggest that Rho-kinase inhibitors represent potential pharmacological tools for the control of asthma.

asthma; guinea pigs; Rho-associated kinases

ASTHMA IS AN INFLAMMATORY pulmonary disease characterized by airway hyperresponsiveness and inflammation, which may be increased by inflammatory mediators, neurotransmitters and inhaled contractile stimuli such as allergens and irritant air pollutants (8). These processes lead to cellular and structural changes in the airways, known as airway remodeling (24, 32, 47).

The most important medications for the control of asthma are the inhaled corticosteroids. However, these drugs present several deficiencies, including heterogeneous individual patient responses and the presence of steroid-resistant processes in airway inflammation (8). Furthermore, the corticosteroids are ineffective in reversing airway remodeling and its functional consequences, including a large effect on airway hyperresponsiveness (7). In this context, there is a growing need for new alternative therapeutic agents that better regulate the various processes involved in the pathophysiology of asthma.

Y-27632 [(+)-(R)-*trans*-4-(1-aminoethyl)-*N*-(4-pyrydil) cyclohexanecarboxamide monohydrate] is an investigational new drug for the treatment for asthma. Y-27632 is a highly selective inhibitor of the Rho-kinase pathway that reverses G protein sensitization and consequently relaxes the airway smooth muscle (17, 45).

Ca^{2+} sensitization, also observed in the airways, is the increase in smooth muscle tension and/or phosphorylation of the 20-kDa regulatory light chain of myosin (MLC_{20}) at a constant Ca^{2+} concentration (51). This Ca^{2+} sensitization is mediated in a variety of smooth muscles by a small G protein, RhoAp21, and its target protein, Rho-kinase (45), which is especially important during the sustained phase of contraction in smooth muscle (51).

Several studies have shown that the use of Rho-kinase inhibitors may be beneficial for the treatment of airway diseases. Experimentally, Rho-kinase appears to be involved in processes such as modulating the degree (and perhaps the development) of airway hyperresponsiveness (15, 38, 40), the infiltration of inflammatory cells into the airways (38, 43), and the growth factor-dependent contraction of human airway smooth muscle (9). These beneficial effects suggest that the inhibition of Rho-kinase signaling may represent a new strategy for resolving airflow limitations in asthma (51).

The aim of the present study was to evaluate the impact of the use of repeated treatment with inhaled Y-27632 on airway hyperresponsiveness, oxidative stress activation, airway extracellular matrix remodeling, eosinophilic inflammation, and T helper (Th)2 and Th1 cytokine expression in an animal model of chronic airway inflammation.

Address for reprint requests and other correspondence: Iolanda de Fátima Lopes Calvo Tibério, Departamento de Clínica Médica, Faculdade de Medicina da Universidade de São Paulo, Av. Dr. Arnaldo, 455 - Sala 1216, CEP: 01246-903, São Paulo, SP, Brazil (e-mail: iocalvo@uol.com.br).

MATERIALS AND METHODS

Animals. We selected 3-wk-old, pathogen-free male Hartley guinea pigs (GP) with initial weights of 300–350 g as subjects for this study. The animals received humane care in compliance with National Institutes of Health guidelines for care and use of laboratory animals. All protocols and procedures described in this study were approved by the Institutional Review Board of The University of São Paulo (São Paulo, SP, Brazil).

Experimental groups. The experimental protocol included four groups ($n = 8$ for each group): *1*) SAL, subjected to the inhalation of aerosolized normal saline; *2*) OVA, exposed to the ovalbumin solution challenge; *3*) SAL-RHO, subjected to the inhalation of aerosolized normal saline and aerosolized Y-27632, starting with the fifth inhalation of saline; and *4*) OVA-RHO, exposed to the ovalbumin solution challenge and aerosolized Y-27632, starting with the fifth inhalation of ovalbumin.

Induction of chronic allergic pulmonary inflammation. The induction of chronic airway inflammation was conducted as described previously (3, 23, 29, 30, 35, 44). In short, the animals were individually placed in a Plexiglas box (30 cm × 15 cm × 20 cm) coupled to an ultrasonic nebulizer (Soniclear, São Paulo, Brazil). An aerosol of ovalbumin solution (Sigma Chemical, St. Louis, MO) diluted in a sterile 0.9% NaCl solution (saline) was generated for 15 min or until respiratory distress occurred. The time that the GP were in contact with the aerosol was termed "inhalation time". A protocol of seven inhalations was conducted twice a week over a period of 4 wk, with increasing concentrations of ovalbumin (1–5 mg/ml) to avoid the development of tolerance. In the first 2 wk (challenges 1–4), the dose of ovalbumin used was 1.0 mg/ml. In the third week (the 5th and 6th challenges), the animals received a solution containing 2.5 mg/ml of ovalbumin. In the last week of the protocol (the 4th wk; the 7th challenge), the dose was increased to 5.0 mg/ml of ovalbumin. The control animals (the SAL group) were subjected to the same protocol with aerosolized saline; see Fig. 1 (44).

Y-27632 treatment. Starting on the fifth inhalation of the experimental protocol, the GP were exposed to 2 min of inhalation with 1 mM Y-27632 (Tocris Bioscience, Ellisville, MO) 10 min before each challenge with ovalbumin or normal saline inhalation. This protocol was based on a previous report stating that 2-min inhalation of 1 mM Y-27632 was capable of inhibiting an acetylcholine-induced increase in lung resistance without altering mean blood pressure (17). The authors administered acetylcholine 10 min after the inhalation of Y-27632 and verified that, 1 h after the inhalation of the drug, its effect on lung resistance was already present. We did not use Y-27632 by intravenous injection at a higher concentration because Uehata et al. (45) reported that this protocol can decrease mean blood pressure in hypertensive rats. In our study, on the day of the mechanical evaluation, Y-27632 inhalation was performed 1 h before the start of the experiment. We elected to administer the drug via inhalation due to its direct effect on the respiratory system and to minimize systemic effects.

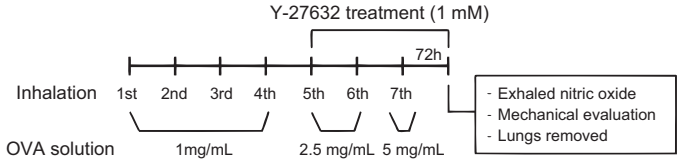

Fig. 1. Timeline of the experimental protocol. The guinea pigs were exposed to 7 inhalations of ovalbumin solution with increasing doses of antigen or normal saline, 2 times per week, for 4 wk. From the 1st to the 4th inhalations, the dose of antigen used was 1 mg/ml; in the 5th and 6th inhalations, the dose was 2.5 mg/ml, and in the 7th inhalation, the dose of antigen used was 5 mg/ml. The ovalbumin or saline solutions were continuously aerosolized for either 15 min or until the onset of respiratory distress. Y-27632 treatment was performed by inhalation of the drug for 2 min at 10 min before each inhalation with ovalbumin (OVA-RHO group) or normal saline (SAL-RHO group), starting with the 5th inhalation. 72 h after the last inhalation, the animals were anesthetized, tracheotomized, and subjected to exhaled nitric oxide (E_{NO}) collection, the evaluation of pulmonary mechanics, and excision of the lungs for the morphometric, histological, and histochemical analyses.

Measurement of E_{NO}. Seventy-two hours after the seventh protocol inhalation and 1 h after the Y-27632 was aerosolized, the GP were anesthetized with pentobarbital sodium (50 mg/kg, intraperitoneal injection), tracheostomized, and mechanically ventilated at 60 breaths/min with a tidal volume of 8 ml/kg using a Harvard 683 ventilator (Harvard Apparatus, Boston, MA). Next, the exhaled nitric oxide (E_{NO}) concentration was measured as described previously (23, 30). In brief, to obtain the E_{NO}, after each animal was stabilized on the ventilator, a collection bag was attached to the expiratory output of the ventilator for 3 min. The E_{NO} was measured using a chemiluminescence technique with a fast-responding analyzer (NOA 280; Sievers Instruments, Boulder, CO). Before each measurement, the analyzer was calibrated with an NO source certified at 47 parts per billion (ppb) (White Martins, São Paulo, Brazil); a zero NO filter (Sievers Instruments) was attached to the inspiratory input to avoid environmental contamination.

Pulmonary mechanics evaluation. After the E_{NO} measurement, a mechanical evaluation was conducted. The tracheal pressure (Ptr) was measured with a 142PC05D differential pressure transducer (Honeywell, Freeport, IL) connected to a side tap in the tracheal cannula. Airflow (V') was obtained using a pneumotachograph (Fleish, Richmond, VA) connected to the tracheal cannula and to a Honeywell 163PC01D36 differential pressure transducer. Lung volume (V) changes were determined by digital integration of the airflow signal. Nine to ten respiratory cycles were averaged to obtain each data point. The Ptr, V', and V signals were collected before and after the SAL or OVA challenge and stored on a microcomputer (30, 35, 36, 44). The baseline measurements of Ptr and V' were performed after the animal was stabilized on the ventilator. Subsequently, 2-min challenges with an aerosol of either ovalbumin (30 mg/mL for the OVA and OVA-RHO groups) or normal saline (for the SAL and SAL-RHO groups) were delivered into the inspiratory circuit through the air inlet of the ventilator. Measurements of Ptr and V' were taken 1 and 3 min after the start of the first challenge. Respiratory system elastance (Ers) and resistance (Rrs) values were obtained using the equation of motion of the respiratory system: $\mathrm{Ptr}(t) = E\mathrm{rs}\cdot\mathrm{V}(t) + R\mathrm{rs}\cdot V'(t)$, where t is time. Immediately after the end of the mechanical evaluation, a positive end-expiratory pressure of 5 cmH_2O was applied to the respiratory system, and the airways were occluded at the end of expiration to maintain the insufflation of the lungs. The GP were then exsanguinated via the abdominal aorta, the anterior chest wall was removed, and the lungs were removed en bloc for morphometric studies and histological analysis.

Morphometric studies. The removed lungs were fixed with buffered 4% paraformaldehyde for 24 h and then transferred to 70% ethanol. Random sections representing peripheral areas of the lungs were processed for paraffin embedding. Histological sections 5 μm thick were obtained. For the immunohistological experiments, the sections were deparaffinized and washed three times for 10 min each with H_2O_2 10V 3% to inhibit endogenous peroxidase activity. Morphometric analysis was performed with a light microscope with an integrating eyepiece (with a reticule with 100 points and 50 lines) using a point-counting technique. As the reticule should be placed adjacent to the airway wall (10), we selected transversely sectioned noncartilaginous airways for analysis. Morphometric analysis of the area of airway wall inflammation was made counting the number of eosinophils or positive cells between the basal membrane of the airway epithelium and the airway smooth muscle. Data did not include the epithelium.

Quantification of eosinophils. For the eosinophil counts, the lungs were stained with Luna's eosinophil granule stain (48). Three airways were randomly selected from each lung section and examined at a

magnification of ×1,000. The number of eosinophils was determined as the number of positive cells in each field divided by the number contacting the airway wall area (10^4 μm^2).

Quantification of collagen and elastic fibers. The lungs were also stained with Picrosirius, a method for collagen identification, and Weigert's Resorcin-Fuchsin, a method for visualizing elastic fibers. Three different airways were randomly selected from each lung to quantify collagen and elastic fiber contents. Quantification was performed by the same method described above. The lung sections were examined at ×1,000 magnification, and the volume proportion of collagen and elastic fibers was determined by dividing the number of points contacting collagen or elastic fibers by the total number of points contacting the tissue in the airway area (between basal membrane of the epithelium and the airway smooth muscle). The results were expressed as percentages.

Evaluation of cytokine-positive cells. For the cytokine evaluations, antigen retrieval was performed with citrate solution for 30 min. Sections were incubated with anti-IL-2, anti-IL-4, anti-IL-5, and anti-IL-13 (all from Santa Cruz Biotechnology, Santa Cruz, CA) and left overnight at 48°C diluted in BSA in the proportions 1:200 (IL-5 and IL-13), 1:400 (IL-2), or 1:500 (IL-4). An ABC Vectastain Kit (Vector Laboratories, Burlingame, CA) was used as the secondary antibody, and 3,3′-diaminobenzidine (DAB) (Dako Cytomation, Carpinteria, CA) was used as a chromogen. The sections were counterstained with Harris hematoxylin (Merck, Darmstadt, Germany). Three airways were analyzed per lung at a magnification of ×1,000, as described above. The positive cells were expressed in cells/unit area (10^4 μm^2).

Evaluation of iNOS. To detect inducible NO synthase (iNOS) activity, immunohistochemistry was performed using a labeled streptavidin-biotin (LSAB) method to visualize iNOS antibody. The antigen retrieval was performed at high temperature in a citrate buffer at pH 6.00. After this treatment, the sections were washed in PBS. Sections were incubated with primary iNOS antibody diluted 1:400 (LabVision; NeoMarkers, Fremont, CA) and incubated overnight. The sections were then washed in PBS and incubated with rabbit IgG using the ABCElite Kit (PK-6101; Vector Laboratories). Next, the sections were again washed, and 3,3′-DAB (Dako Cytomation) was used as a chromogen. The sections were washed in flowing water and counterstained with Harris hematoxylin (Merck). Three airways per lung were analyzed at a magnification of ×1,000, as previously described. The number of iNOS-positive cells was determined as the number of positive cells in each field divided by the number contacting the airway wall area (10^4 μm^2).

Evaluation of 8-isoprostane-PGF2α. Immunohistochemical staining was performed using an antibody to anti-8-epi-prostaglandin F (PGF)2α (Oxford Biomedical Research, Rochester Hills, MI) at a 1:500 dilution. Antigen retrieval was performed with trypsin for 20 min. Subsequently, three washes in PBS were performed for 3 min each. Sections were incubated with anti-8-epi-PGF2α (1:500) diluted in BSA overnight. After washes in PBS, the ABC Vectastain kit (Vector Laboratories) was used to provide a secondary antibody, and 3,3′-DAB (Dako Cytomation) was used as a chromogen. The sections were counterstained with Harris hematoxylin (Merck). The analysis was performed on the slides stained for 8-isoprostane by applying the same point-counting technique described above. We determined the volume proportion of 8-iso-PGF2α in the airway wall area as the ratio of the numbers of points falling on 8-iso-PGF2α stained and unstained tissues. The lung sections were examined at a magnification of ×1,000, and the results were expressed as percentages.

Evaluation of actin. The immunohistochemistry to detect actin utilized the LSAB method for the detection of human smooth-muscle actin markers (Dako). Antigen retrieval for the smooth-muscle actin marker was performed at high temperature in a citrate solution at pH 6.0 for 30 min. After this treatment, the sections, still immersed in the same solution, were cooled to room temperature for 20 min and washed in PBS three times. Before the incubation with the primary antibody, protein blocking with 2% skim milk was performed for 10 min. The sections were then washed again in PBS and incubated with the LSAB Plus-HRP kit (Dako). The chromogen used was again 3,3′-DAB (Dako). Finally, the sections were washed in water and counterstained with Harris hematoxylin (Merck). Analyses were performed by applying the same point-counting technique described above. The proportion of actin in the area of the airway wall was obtained as the ratio between the numbers of coinciding points on actin and unstained tissue. The sections were examined at a magnification of ×1,000, and the results were expressed as percentages.

Evaluation of TIMP-1. The immunohistochemistry used for the tissue inhibitor of metalloproteinase (TIMP)-1 assay utilized the peroxidase enzyme. Antigen retrieval was performed at a high temperature in a citrate buffer at pH 6.0 for 1 min. After this treatment, the sections were washed in flowing water, distilled water, and PBS. Subsequently, endogenous peroxidase blocking was performed with methanol V/V and H_2O_2 10V 3% for 10 min and then with H_2O_2 10V 3% only three times for 5 min each. The sections were then washed again with flowing water, distilled water, and PBS. After the blocking, a TIMP-1 monoclonal antibody (Lab Vision) diluted 1:50 in BSA was applied to the sections and incubated from 2°C to 8°C overnight for at least 12 h. The sections were then washed in PBS and incubated with the Novolink Polymer Kit (Novocastra, Newcastle, UK). After this step, the sections were washed in PBS and 3,3′-DAB (Sigma Chemical) was used as a chromogen. Finally, the sections were washed with water and counterstained with Harris hematoxylin (Merck). Three airways were analyzed per lung at a magnification of ×1,000, as described above. The number of positive cells was expressed as cells/unit area (10^4 μm^2).

Evaluation of MMP-9, TGF-β, NF-κB, and IFN-γ. The immunohistochemistry to detect cells expressing matrix metalloproteinase (MMP)-9, transforming growth factor (*TGF*)-β, NF-κB, and IFN-γ followed procedures similar to those described above using the LSAB method. Antigen retrieval was achieved at a high temperature. After this treatment, the sections were washed in flowing water, deionized water, and PBS. After blocking, primary monoclonal antibodies diluted in BSA were applied over the sections in the following ratios and incubated overnight: MMP-9, 1:500 (Lab Vision); *TGF*-β, 1:1,500 (Santa Cruz Biotechnology); NF-κB, 1:50 (Santa Cruz Biotechnology); and IFN-γ, 1:50 (Santa Cruz Biotechnology). The sections were then washed in PBS and incubated. After this step, the sections were washed in PBS and visualized with the 3,3′-DAB chromogen (Dako Cytomation). Finally, the sections were washed in flowing water and counterstained with Harris hematoxylin (Merck). Three airways were analyzed per lung at a magnification of ×1,000, as described above. The number of positive cells was expressed as cells/unit area (10^4 μm^2).

Passive cutaneous anaphylaxis. For the titration of the IgG1 and IgE antibodies, we used the technique of Ovary (1964) as modified by Mota and Perini (28). Three GP from each group were anesthetized with pentobarbital sodium (50 mg/kg ip), and 5 ml of blood was drawn by cardiac puncture. The blood was centrifuged at 1,000 rpm for 20 min at a temperature of 4°C. For the IgG1 titration, a portion of the sample was heated in a water bath at 56°C for 1 h to inactivate IgE antibodies. The backs of the GP were trichotomized, taking care to not irritate the skin. Aliquots of 0.1 ml of each concentration of serum (from 1:5 to 1:2,560) were injected into the dorsal subcutaneous tissues of the GP. After 24 h for IgG1 and 10 days for IgE, a solution containing 1 mg of ovalbumin, 1 mg of Evans blue, and 0.25% saline was injected into the bloodstream. After 30 min, the animals were killed, their skin removed and inverted, and the diameters of the reactions were analyzed, with reactions larger than 5 mm in diameter considered to be positive. The titer was determined as the highest dilution of serum that induced a passive cutaneous anaphylactic reaction.

Statistical analysis. All data are reported as the means ± SE. The statistical significance of differences between groups was determined by ANOVA followed by the *Holm-Sidak* method for multiple com-

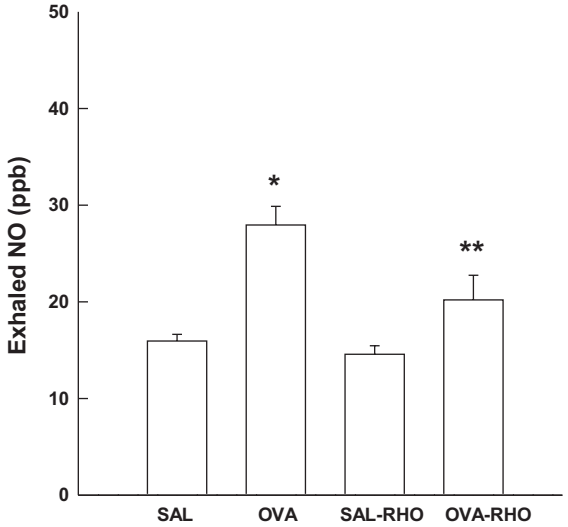

Fig. 2. Vertical bar graph representing the means ± SE of the E_{NO} concentrations of the anesthetized guinea pigs. The E_{NO} was collected 72 h after the 7th inhalation (before the challenge) with saline or OVA solutions in the 4 experimental groups. *$P < 0.05$ compared with the other groups; **$P < 0.05$ compared with OVA group.

parisons. We also obtained the Pearson correlation coefficient (R) to assess the associations of the Rrs and Ers scores with the markers for remodeling, inflammatory cells, and oxidative stress. All statistical analysis was performed using SigmaStat software (Systat Software, San Diego, CA). Differences were considered significant when $P < 0.05$.

RESULTS

Inhalation time. There were no differences in the inhalation times among the groups studied until the fourth inhalation, and all animals reached 15 min of inhalation. None of the normal saline groups (SAL and SAL-RHO groups) presented respiratory distress during the seven inhalations. From the fifth to seventh inhalation, sensitized and untreated animals (the OVA group) presented lower inhalation times compared with the group that was sensitized and treated with Y-27632 (OVA-RHO group) (8.87 ± 2.59 min and 12.52 ± 2.9 min, respectively; $P < 0.05$).

E_{NO}. Figure 2 presents the levels of E_{NO} measured at 72 h after the last inhalation with saline or OVA challenge. The concentrations of E_{NO} were higher in the OVA group (27.9 ± 1.92 ppb) than in the SAL (15.9 ± 0.69 ppb) and SAL-RHO (14.5 ± 0.88 ppb) groups ($P < 0.001$). The treatment with Y-27632 reduced the E_{NO} of the OVA-RHO group (20.2 ± 2.55 ppb) compared with the OVA group ($P < 0.05$).

Table 1. *Baseline values of the Rrs and Ers among the experimental groups*

Group	Rrs, $cmH_2O \cdot ml^{-1} \cdot s$	Ers, cmH_2O/ml
SAL	0.23 ± 0.01	2.64 ± 0.16
OVA	0.20 ± 0.02	2.50 ± 0.22
SAL-RHO	0.11 ± 0.01	2.23 ± 0.10
OVA-RHO	0.25 ± 0.05	1.82 ± 0.22

Values are means ± SE. SAL, saline group; OVA, ovalbumin group; RHO, Rho-kinase group; Rrs, respiratory system resistance; Ers, respiratory system elastance.

Pulmonary mechanical evaluation. There were no differences in the baseline values of the respiratory system resistance and elastance among the experimental groups (see Table 1). The percentage of maximal increase of Rrs is illustrated in Fig. 3*A*. There was a significant increase of %Rrs in the OVA group (141.86 ± 6.6%) compared with the controls (SAL group: 7.99 ± 1.66%; SAL-RHO group: 6.2 ± 2.74%). The treatment of sensitized animals with the Rho-kinase inhibitor attenuated this response (OVA-RHO group: 7.68 ± 2.69%; $P < 0.001$).

The percentage of maximal increase of Ers is shown in Fig. 3*B*. There was also a significant increase of %Ers in the OVA group (10.88 ± 2.12%) compared with the control groups (SAL: 3.20 ± 0.19%; SAL-RHO: 2.39 ± 0.13%). The inhibition of Rho-kinase reduced this response compared with the OVA group (OVA-RHO group: 2.28 ± 0.21%; $P < 0.001$).

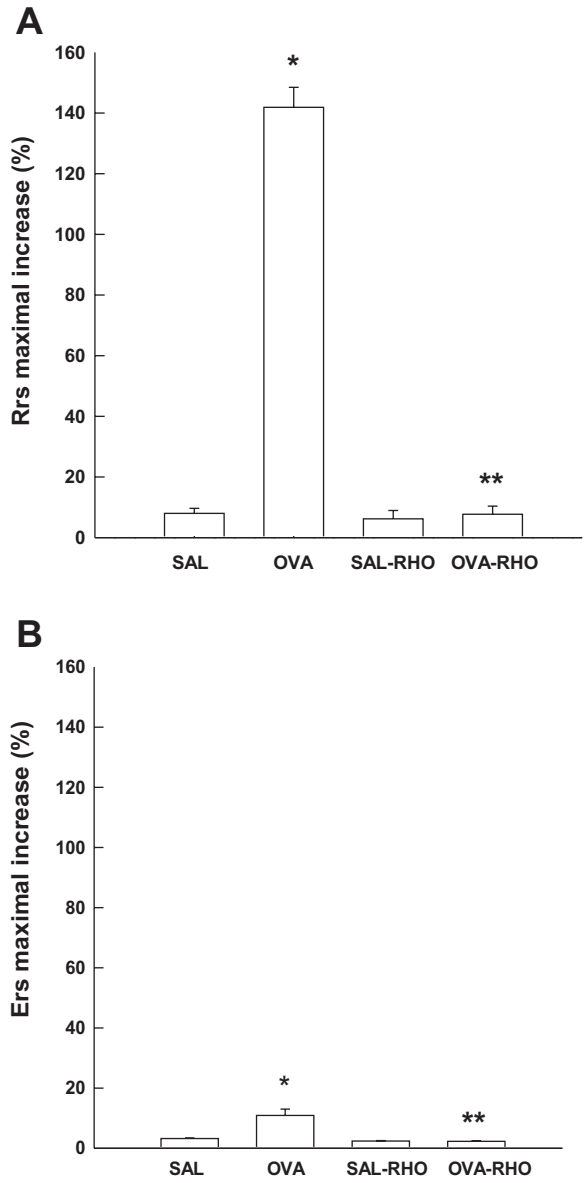

Fig. 3. Vertical bar graph showing the means ± SE of the maximal percentage increases in respiratory system resistance (Rrs) (*A*) and elastance (Ers) (*B*) obtained after airway challenge with ovalbumin (30 mg/ml) or normal saline in anesthetized guinea pigs. *$P < 0.001$ compared with the SAL, SAL-RHO, and OVA-RHO groups; **$P < 0.001$ compared with the OVA group.

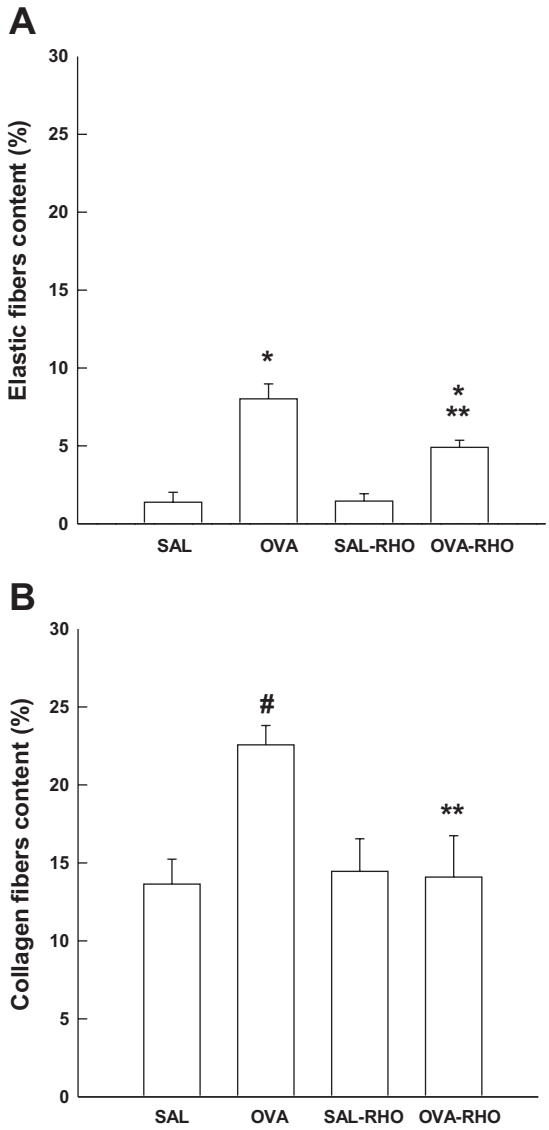

Fig. 4. Vertical bar graph showing the means ± SE of the elastic fiber (*A*) and collagen (*B*) contents for the 4 experimental groups. The results are expressed as percentages. *$P < 0.05$ compared with the SAL and SAL-RHO groups; **$P < 0.05$ compared with the OVA group; and #$P < 0.05$ compared with all other groups.

Thinking that the effects of Y-27632 on airway responsiveness could be an acute effect, we chose to create one more experimental group. This new group (OVA-wfRHO = OVA-without final RHO) followed the same protocol of the preceding groups but did not receive the last inhalation of the inhibitor (performed until 1 h before lung mechanics evaluation). The difference was maintained in *%R*rs OVA-wfRHO group (21.47 ± 5.71%) compared with OVA group ($P < 0.001$). The *%E*rs difference between the OVA-wfRHO group (2.53 ± 0.38%) and OVA group also remained ($P < 0.001$).

Morphometric analysis. The volume proportion of elastic fibers is illustrated in Fig. 4*A*. The elastic fiber contents were higher in the OVA-exposed animal groups (OVA: 8.01 ± 0.63%; and OVA-RHO: 4.09 ± 0.45%) compared with the saline-exposed GP (SAL group: 1.38 ± 0.63%; SAL-RHO group: 1.45 ± 0.47%; $P < 0.001$). The animals treated with Y-27632 presented lower elastic fiber contents than the sensitized and untreated animals (OVA-group; $P < 0.05$).

There was an increase in the collagen contents in the airways of the ovalbumin-exposed GP (OVA: 22.57 ± 1.24%; OVA-RHO: 14.09 ± 2.65%) compared with the saline-exposed ones (SAL: 13.64 ± 1.59%; SAL-RHO: 14.45 ± 2.09%). The treatment with Y-27632 also attenuated the collagen fiber content in the ovalbumin-exposed animals ($P < 0.05$). These data are presented in Fig. 4*B*.

Figure 5 shows the values of eosinophil density in the airways of the four experimental groups. We observed an increase in eosinophil density in the ovalbumin-exposed GP (OVA: 27.42 ± 4.95 cells cells/10^4 μm^2) compared with the controls (SAL: 6.67 ± 1.38 cells/10^4 μm^2; SAL-RHO: 4.57 ± 0.44 cells/10^4 μm^2; $P < 0.001$). The treatment with the Rho-kinase inhibitor reduced the numbers of these cells in the animals exposed to ovalbumin challenge (OVA-RHO: 13.26 ± 1.39 cells/10^4 μm^2; $P < 0.05$). The values of eosinophil density were also verified for the OVA-wfRHO group, and the difference to OVA group was retained ($P < 0.05$).

Figure 6*A* presents the numbers of IL-2-positive cells for all experimental groups. There was increase in IL-2-positive cells in the airways of the untreated ovalbumin-sensitized animals (the OVA group: 33.07 ± 0.72 cells/10^4 μm^2) compared with the groups exposed to inhalation with saline solution (SAL group: 2.86 ± 0.72 cells/10^4 μm^2; SAL-RHO group: 6.70 ± 1.12 cells/10^4 μm^2; $P < 0.001$). The number of IL-2-positive cells in the OVA-exposed group that was also treated with Y-27632 was reduced (OVA-RHO group: 11.08 ± 0.87 cells/10^4 μm^2; $P < 0.001$).

We also observed (Fig. 6*B*) an increase in the number of IL-4-positive cells in untreated animals exposed to ovalbumin challenges (OVA group: 14.44 ± 1.16 cells/10^4 μm^2) compared with the animals of the control groups (SAL: 3.19 ± 0.90 cells/10^4 μm^2; SAL-RHO: 2.59 ± 0.74 cells/10^4 μm^2) and the treated group (OVA-RHO: 8.53 ± 1.13 cells/10^4 μm^2), for which we observed an attenuation of the IL-4-positive cell

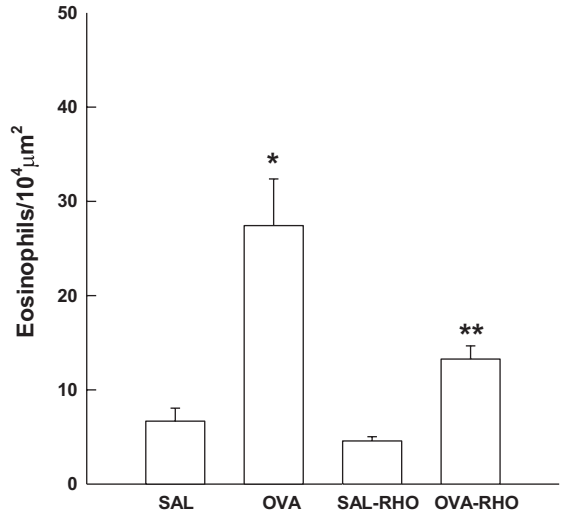

Fig. 5. Vertical bar graph showing the means ± SE of the eosinophil densities in the lungs of the animals exposed to inhalations with ovalbumin or normal saline and treated with Rho-kinase inhibitor or vehicle. *$P < 0.05$ compared with the SAL, SAL-RHO, and OVA-RHO groups; **$P < 0.001$ compared with OVA group.

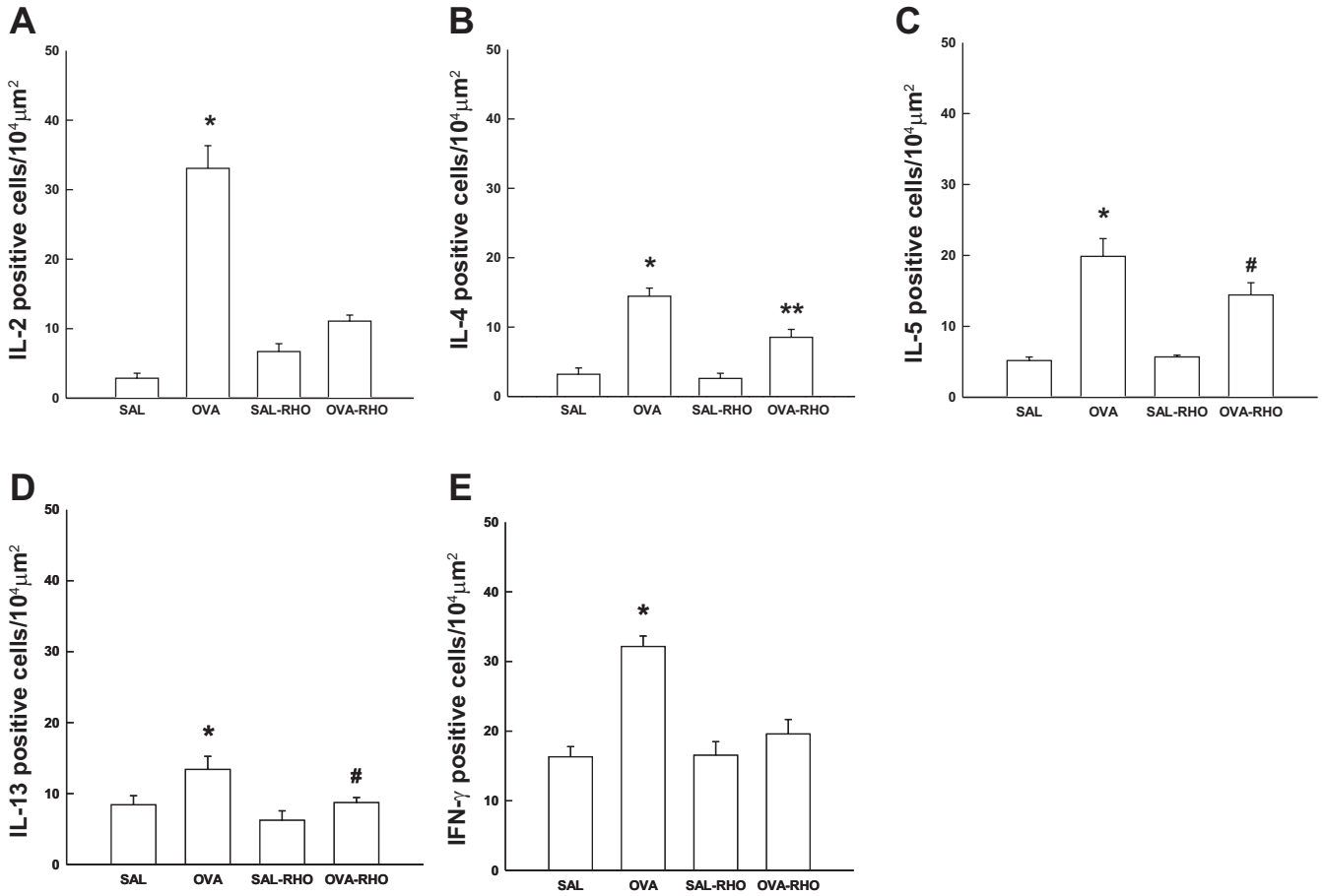

Fig. 6. Vertical bar graph showing the means ± SE of the cytokine-positive cells in the airways of the animals; IL-2 (*A*), IL-4 (*B*), IL-5 (*C*), IL-13 (*D*), and IFN-γ (*E*). The untreated ovalbumin-exposed animals had greater numbers of all types of interleukin-positive cells than those in the other groups. Treatment with the Rho-kinase inhibitor attenuated the numbers of Il-2-, IL-4-, IL-5-, and IL-13-positive cells in the airway wall areas. *$P < 0.05$ compared with the other groups; **$P < 0.001$ compared with OVA group; and #$P < 0.05$ compared with the OVA group.

counts ($P < 0.001$). Despite this attenuation of the number of IL-4-positive cells in the treated animals, there was a difference in the values of this group in relation to the control group ($P < 0.001$).

Figure 6*C* shows the number of IL-5-positive cells in the airways of the GP of the four experimental groups. We observed an increase in the number of IL-5-positive cells in the airways of the ovalbumin-sensitized animals (OVA group: 19.86 ± 2.49 cells/10^4 μm^2 and OVA-RHO group: 14.42 ± 1.71 cells/10^4 μm^2) compared with the controls (SAL group: 5.17 ± 0.50 cells/10^4 μm^2; SAL-RHO group: 5.68 ± 0.25 cells/10^4 μm^2; $P < 0.001$). We observed reduced numbers of IL-5-positive cells in the airways of the GP sensitized to ovalbumin and treated with Y-27632 in relation to the OVA group animals ($P < 0.05$), although there was a significant difference between the treated animals and the control group ($P < 0.001$).

The numbers of IL-13-positive cells are illustrated in Fig. 6*D*. The group of GP exposed to ovalbumin presented a higher number of IL-13-positive cells (OVA: 13.39 ± 1.85 cells/10^4 μm^2) than the groups exposed to saline (SAL: 8.40 ± 1.28 cells/10^4 μm^2; SAL-RHO: 6.22 ± 1.34 cells/10^4 μm^2; $P < 0.05$). Ovalbumin-exposed GP that received treatment with the Rho-kinase inhibitor presented a reduced number of IL-13-positive cells (OVA-RHO group: 8.71 ± 0.72 cells/10^4 μm^2) compared with the OVA group ($P < 0.05$).

We also observed (Fig. 6*E*) an increase in the number of cells positive for IFN-γ in the untreated animals exposed to ovalbumin challenges (OVA group: 32.14 ± 1.5 cells/10^4 μm^2) compared with the control groups (SAL: 16.31 ± 1.46 cells/10^4 μm^2; RHO-SAL: 16.53 ± 1.94 cells/10^4 μm^2) and the group treated with the Rho-kinase inhibitor (OVA-RHO: 19.58 ± 2.09 cells/10^4 μm^2), for which we observed an attenuation of IFN-γ-positive cells ($P < 0.001$).

The measurements of the iNOS-positive cells are presented in Fig. 7*A*. The number of iNOS-positive cells was significantly higher in the untreated ovalbumin-exposed animals (OVA group: 14.69 ± 1.09 cells/10^4 μm^2) compared with the saline-exposed animals (SAL group: 9.65 ± 1.37 cells/10^4 μm^2; SAL-RHO group: 9.05 ± 0.7 cells/10^4 μm^2; $P < 0.05$) and the Y-27632-treated animals exposed to ovalbumin (OVA-RHO group: 10.37 ± 0.68 cells/10^4 μm^2; $P < 0.05$).

The volume proportions of 8-iso-PGF2α in the airways of the GP are illustrated in Fig. 7*B*. We observed increased 8-iso-PGF2α contents in the airways of the OVA-exposed animals groups (OVA: 25.93 ± 1.62%) compared with the saline-exposed guinea pigs (SAL group: 16.55 ± 2.33%; SAL-RHO group: 15.73 ± 1.89%; $P < 0.05$). The animals

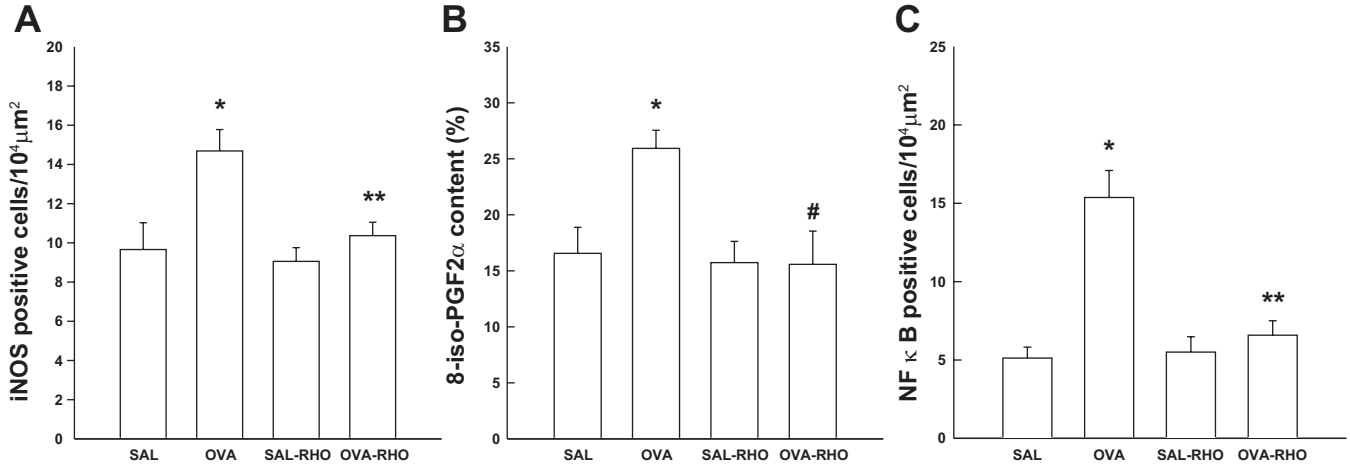

Fig. 7. Vertical bar graph showing the means ± SE of the numbers of cells positive for the expression of inducible nitric oxide synthase (iNOS) (*A*), 8-isoprostane-prostaglandin F(PGF)2α (*B*), and NF-κB (*C*) present in the airways of guinea pigs from all the experimental groups. *$P < 0.05$ compared with the SAL, SAL-RHO, and OVA-RHO groups; **$P < 0.001$ compared with the OVA group; and #$P < 0.05$ compared with the OVA group.

treated with Y-27632 presented lower contents of 8-iso-PGF2α (OVA-RHO group: 15.58 ± 2.97%) compared with both the sensitized and untreated animals.

The numbers of NF-κB-positive cells are presented in Fig. 7*C*. The numbers of NF-κB-positive cells were significantly higher in the untreated animals exposed to ovalbumin (OVA group: 15.37 ± 1.72 cells/10^4 μm^2) than in the groups exposed to saline (SAL: 5.12 ± 0.69 cells/10^4 μm^2; SAL-RHO: 5.05 ± 0.9 cells/10^4 μm^2; $P < 0.001$) and the ovalbumin-exposed animals treated with Y-27632 (OVA-RHO group: 6.58 ± 0.92; $P < 0.001$).

There was also statistically significant differences of smooth-muscle-specific actin present in the airway walls between groups. We observed increased smooth-muscle-specific actin contents in the airways of the ovalbumin-exposed animals groups (OVA: 25.75 ± 1.31%) compared with the saline-exposed GP (SAL group: 9.84 ± 1%; SAL-RHO group: 9.94 ± 0.9%; $P < 0.001$). and with the sensitized and treated animals (OVA-RHO group: 12.16 ± 0.69%; $P < 0.001$).

The numbers of MMP-9-positive cells are shown in Fig. 8*A*. There was a significant increase in the number of MMP-9-positive cells in the OVA group (24.01 ± 0.90 cells/10^4 μm^2) compared with the controls (SAL group: 14.09 ± 1.25 cells/10^4 μm^2; SAL-RHO group: 12.89 ± 1.7 cells/10^4 μm^2; $P < 0.001$). The treatment of the sensitized animals with the Rho-kinase inhibitor attenuated this response (OVA-RHO group: 13.20 ± 1.96; $P < 0.001$).

Figure 8*B* presents the numbers of TIMP-1-positive cells for all experimental groups. The number of cells positive for TIMP-1 also increased in the airways of the untreated animals exposed to ovalbumin (OVA group: 15.52 ± 2.63 cells/10^4 μm^2) compared with the groups exposed to inhaled saline (SAL group: 5.79 ± 1.01 cells/10^4 μm^2; SAL-RHO group: 4.71 ± 0.76 cells/10^4 μm^2; $P < 0.001$). The number of TIMP-1-positive cells in the group exposed to OVA but treated with Y-27632 was reduced (OVA-RHO group: 9.03 ± 0.53 cells/10^4 μm^2; $P < 0.05$).

The number of TGF-β-positive cells is shown in Fig. 8*C*. The group of GP exposed to ovalbumin showed a higher number of cells positive for TGF-β (OVA group: 10.8 ± 0.54 cells/10^4 μm^2) than the groups exposed to saline (SAL: 6.95 ±

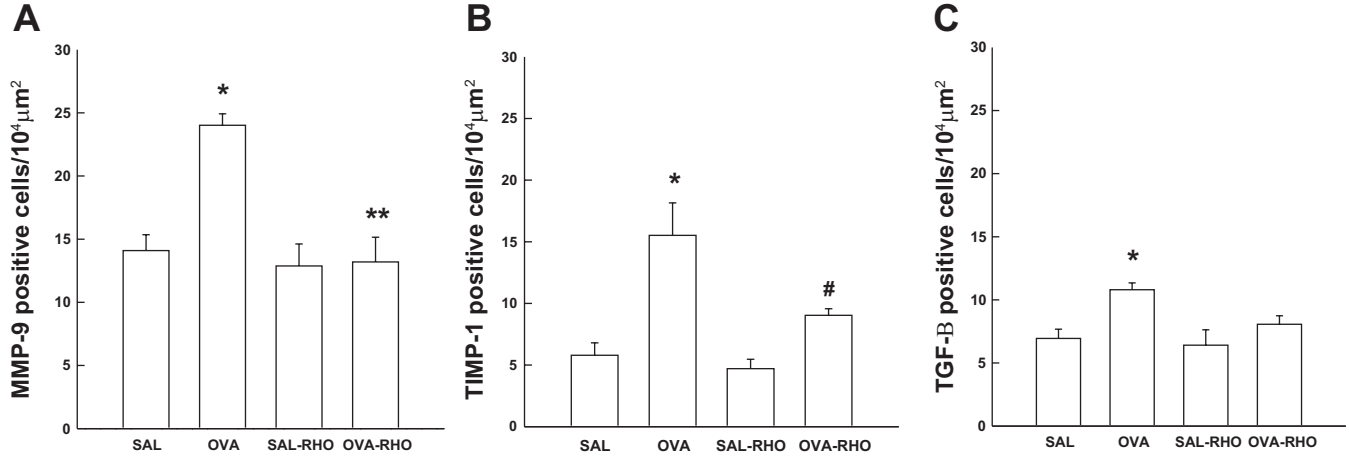

Fig. 8. Vertical bar graph showing the means ± SE of the numbers of matrix metalloproteinase (MMP)-9- (*A*), tissue inhibitor of metalloproteinase (TIMP)-1- (*B*), and TGF-β-positive cells (*C*) in the airways of guinea pigs exposed to 7 inhalations with saline or ovalbumin and repeatedly treated with Y-27632 or vehicle. The results are expressed as percentages. *$P < 0.05$ compared with the other groups; **$P < 0.001$ compared with the OVA group; and #$P < 0.05$ compared with the OVA group.

0.73 cells/10^4 μm^2; SAL-RHO: 6.14 ± 1.21 cells/10^4 μm^2; $P < 0.05$). The GP exposed to ovalbumin and treated with the Rho-kinase inhibitor showed a decreased number of TGF-β-positive cells (OVA-RHO group: 8.07 ± 0.67 cells/10^4 μm^2) compared with the OVA group ($P < 0.05$).

Table 2 presents the correlations of *R*rs and *E*rs with the measures for inflammatory cells, remodeling markers, and oxidative stress markers. We observed significant correlations among all the parameters evaluated. In relation to the passive cutaneous anaphylaxis (PCA), there were no detectable IgG1 antibodies in the SAL and SAL-RHO groups. The PCA showed an increase in specific anaphylactic IgG1 antibodies in GP exposed to ovalbumin (OVA group; maximum titration, 1:640). This response was reduced in the animals treated with Y-27632 (OVA-RHO group; maximum titration, 1:160).

Figure 9 shows representative photomicrographs of GP airways stained for cells expressing IL-2, IL-4, IL-5, and IL-13. The untreated GP subjected to ovalbumin challenge (OVA group) presented prominent increases in the numbers of all cytokine-positive cells (Fig. 9, *B*, *F*, *J*, and *N*) compared with the unsensitized animals (SAL group: Fig. 9, *A*, *E*, *I*, and *M*; SAL-RHO group: Fig. 9, *C*, *G*, *K*, and *O*) and the animals in the OVA-RHO group (Fig. 9, *D*, *H*, *L*, and *P*) receiving treatment with the Rho-kinase inhibitor.

Representative photomicrographs of the airways of the animals stained with Picrosirius for collagen content, Weighert Resorcin-Fuchsin for elastic fiber content, and immunohistochemistry for the volume proportions of actin and 8-iso-PGF2α are shown in Fig. 10. Except for actin content, for which no difference was found among the groups, all the other fiber contents were elevated in the untreated ovalbumin-exposed animals (OVA group; Fig. 10, *B*, *F*, *J*, and *N*) compared with the saline-exposed animals (SAL group; Fig. 10, *A*, *E*, *I*, and *M*; SAL-RHO group; Fig. 10, *C*, *G*, *K*, and *O*). The treatment of the GP exposed to ovalbumin with the Rho-kinase inhibitor reduced the contents of collagen fibers (Fig. 10*D*), elastic fibers (Fig. 10*H*), and 8-iso-PGF2α (Fig. 10*L*).

Figure 11 presents photomicrographs of airway walls from GP in the four experimental groups subjected to Luna staining for the detection of eosinophil density and immunohistochemical staining for iNOS, NF-κB, and IFN-γ detection. The animals exposed to ovalbumin (the OVA group) presented intense eosinophilic infiltration (Fig. 11*B*) and increased numbers of iNOS- (Fig. 11*F*), NF-κB- (Fig. 11*J*), and IFN-γ- (Fig. 11*N*) positive cells compared with the saline-exposed animals (SAL group; Fig. 11, *A*, *E*, *I*, and *N*; SAL-RHO group; Fig. 11, *C*, *G*, *K*, and *O*). Treatment with Y-27632 decreased the degree of eosinophilic infiltration (Fig. 11*D*) and the numbers of iNOS- (Fig. 11*H*), NF-κB- (Fig. 11*L*), and IFN-γ- (Fig. 11*P*) positive cells in the ovalbumin-exposed GP.

Representative photomicrographs of immunohistochemical staining for MMP-9, TIMP-1, and TGF-β in the airways of the four animal groups are shown in Fig. 12. There was an increase in the numbers of MMP-9-, TIMP-1-, and TGF-β-positive cells in the groups of untreated ovalbumin-exposed animals (OVA group; Fig. 12, *B*, *F*, and *J*, respectively) compared with the saline-exposed animals (SAL group; Fig. 12, *A*, *E*, and *I*; and SAL-RHO group; Fig. 12, *C*, *G*, and K). Treatment of the GP exposed to ovalbumin with Y-27632 reduced the numbers of MMP-9- (Fig. 12*D*), TIMP-1 (Fig. 12*H*), and TGF-β- (Fig. 12*L*) positive cells. Note that, although the microscopic analyses were performed at a magnification of ×1,000, we chose to present photomicrographs at lower magnifications to better highlight the differences among the groups.

Table 2. *Pearson correlations of Rrs and Ers with the measures for inflammatory cells, remodeling markers, and oxidative stress markers*

	*R*rs	*E*rs
Inflammatory Cells		
Eosinophils	0.585	0.766
	0.00673	0.0000810
IL-2	0.706	0.897
	0.000509	0.0000000857
IL-4	0.763	0.684
	0.0000910	0.000890
IL-5	0.679	0.495
	0.00100	0.0264
IL-13	0.699	0.510
	0.000605	0.0216
Remodeling markers		
Elastic fibers	0.614	0.667
	0.00394	0.00131
Collagen fibers	0.462	0.595
	0.0402	0.00562
TGF-β	0.625	0.636
	0.00322	0.00259
TIMP-1	0.640	0.756
	0.00237	0.000116
MMP-9	0.795	0.751
	0.0000280	0.000137
Oxidative stress markers		
NF-κB	0.823	0.889
	0.00000846	0.000000166
iNOS	0.794	0.663
	0.0000292	0.00144
NO	0.720	0.828
	0.000346	0.00000643
Isoprostane	0.710	0.687
	0.000457	0.000815

For each data set, the top number is the *r* value, and the bottom is the *P* value. TIMP, tissue inhibitor of metalloproteinase; MMP, matrix metalloproteinase; iNOS, inducible nitric oxide (NO) synthase.

DISCUSSION

In the present study, we evaluated the role of Y-27632, a Rho-kinase inhibitor, on oxidative stress, respiratory system mechanics, inflammation, and extracellular matrix remodeling in the airways of GP with chronic allergic airway inflammation. The results showed that repeated Rho-kinase inhibition reduced the airway mechanical responses to antigenic challenge, with correlated reductions in $E_{NO,}$ eosinophilic infiltration, the numbers of IL-2-, IL-4-, IL-5- and IL-13-positive cells, and extracellular matrix remodeling in the airway wall. Additionally, there was a significant reduction in the activation of the oxidative stress pathway, which was also correlated with the attenuation of the maximum mechanical responses after antigen challenge.

We previously studied this model of chronic allergic pulmonary inflammation in GP, and the present results confirm our previous data, demonstrating that the ovalbumin-sensitized animals required shorter lengths of time in contact with the antigen during the challenges (23, 31, 44). In addition, these previous studies confirmed the presence of airway hyperresponsiveness (23, 30, 31, 35), inflammation (31, 32, 35), and remodeling (30, 32, 35) in the sensitized GP, constituting an

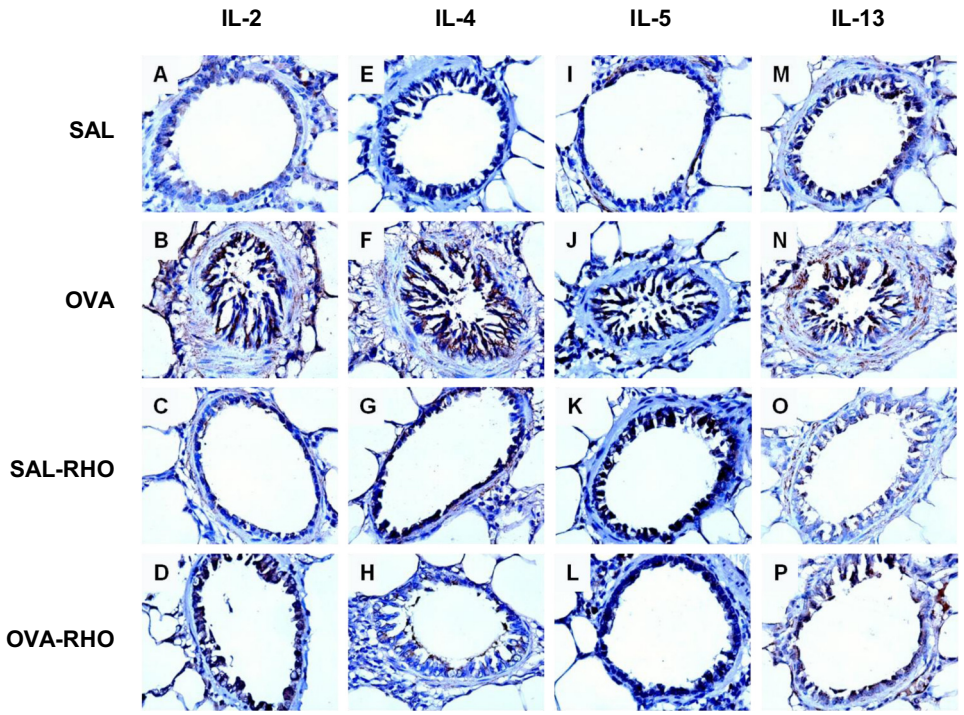

Fig. 9. Photomicrographs of the results of immunohistochemical analyses of airway walls to detect IL-2 (*A–D*, ×400), IL-4 (*E–H*, ×400), IL-5 (*I–L*, ×400), and IL-13 (*M–P*, ×400) from guinea pigs exposed only to saline (*A*, *E*, *I*, and *M*) or ovalbumin (*B*, *F*, *J*, and *N*). The treated guinea pigs exposed to saline (*C*, *G*, *K*, and *O*) or ovalbumin (*D*, *H*, *L*, and *P*) are also represented.

interesting model for the study of possible therapeutic strategies for asthma.

The treatment with the Rho-kinase inhibitor was started on the fifth inhalation to avoid possible interference with the sensitization process. We also previously demonstrated that, at this time, the GP were already sensitized and showed an increase in the level of IgG1-specific anaphylactic antibodies detected using the PCA technique (44). This elevation of IgG1-specific antibodies in ovalbumin-exposed groups was also demonstrated in the present study.

Acute responses to antigen exposure were evaluated by the time that guinea pigs were able to be in contact with the ovalbumin aerosol (inhalation time). In this context, treatment with Rho-kinase inhibitor attenuated this response in the sensitized animals. We reasoned that an acute response to antigen challenge may be related to several mechanisms including

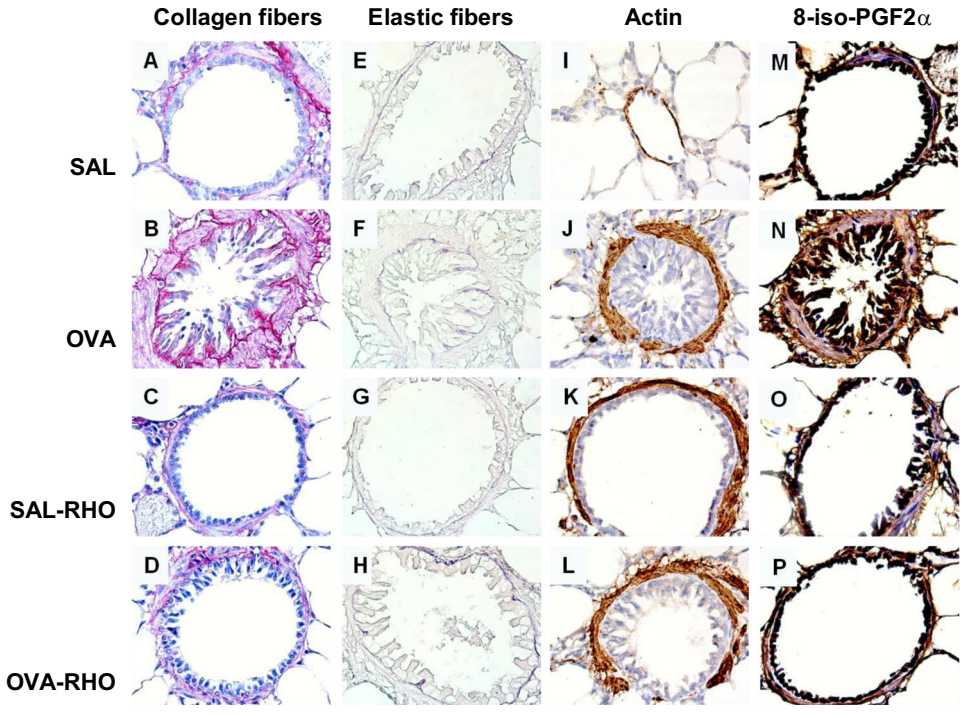

Fig. 10. Representative photomicrographs of guinea pig airways stained with Picrosirius for collagen content (*A–D*, ×400), Weighert Resorcin-Fuchsin for elastic fiber content (*E–H*, ×400), actin (*I–L*, ×400), and 8-iso-PGF2α (*M–P*, ×400). The 4 experimental groups are represented: SAL (*A*, *E*, *I*, and *M*), OVA (*B*, *F*, *J*, and *N*), SAL-RHO (*C*, *G*, *K*, and *O*), and OVA-RHO (*D*, *H*, *L*, and *P*).

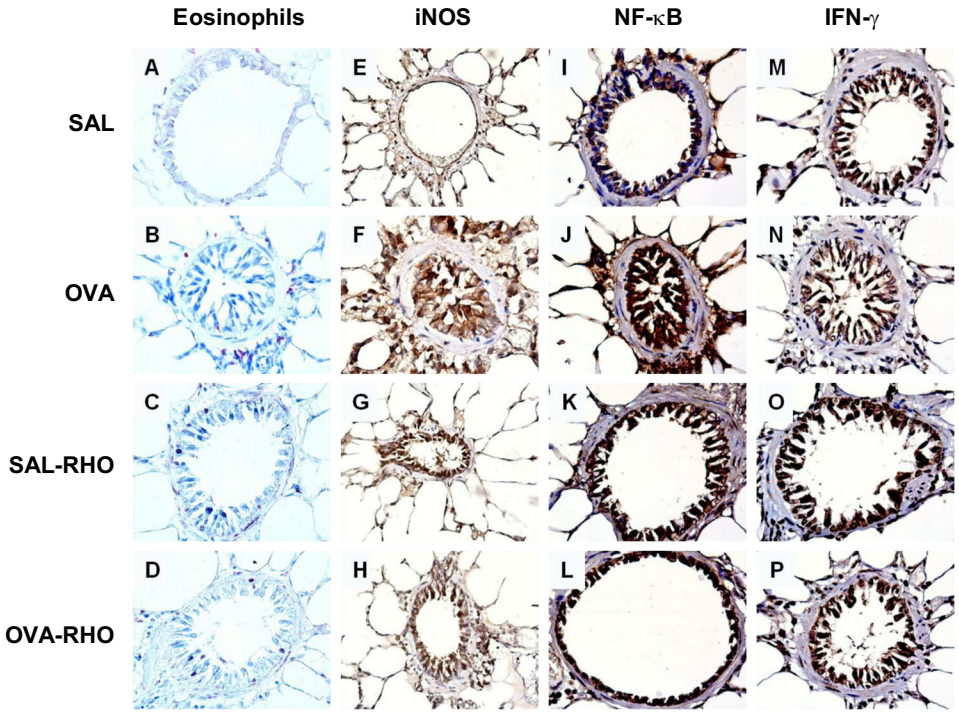

Fig. 11. Representative photomicrographs of guinea pig airways stained with Luna (*A–D*, ×400) and immunohistochemistry results for iNOS (*E–H*, ×400), NF-κB (*I–L*, ×400), and IFN-γ (*M–P*, ×400). All experimental groups are represented: SAL (*A*, *E*, *I*, and *M*), OVA (*B*, *F*, *J*, and *N*), SAL-RHO (*C*, *G*, *K*, and *O*), and OVA-RHO (*D*, *H*, *L*, and *P*).

smooth-muscle responses that were likely modified by Y-27632 treatment.

The repeated treatment with Y-27632 caused a significant decrease in the level of NO exhaled from ovalbumin-sensitized GP. Note that this may have occurred due to the acute effects of Y-27632, used 1 h before E_{NO} measurement.

The E_{NO} is a well-established, noninvasive biomarker of airway inflammation that can be used for the assessment of asthma severity, as elevated E_{NO} levels are associated with continued inflammation both in humans (4, 19) and in animal models (23, 30, 42). The level of NO detected in the exhaled air is traditionally used to evaluate the efficacy of new treatments in experimental models of pulmonary inflammation (32). Interestingly, previous studies have shown that, in the same model of chronic allergic pulmonary inflammation used in this study, NO derived from constitutive isoforms acts as a potent bronchodilator, vasodilator, and protector against collagen fiber deposition around airways and blood vessels (30). Furthermore, when the NO derived from the inducible NO synthase isoform was inhibited exclusively, an attenuation of airway constriction, inflammation, and remodeling processes was noted, reducing both collagen and elastic fiber deposition in airways and distal lung parenchyma, suggesting the contribution of another NO isoform to the pathophysiology of asthma (32, 42).

We also showed that the baseline values of resistance and elastance of the respiratory system in Y-27632-treated and -untreated animals were unaltered. However, the maximal responses to antigen challenge were significantly reduced by Rho-kinase inhibition in the sensitized animals. There is evidence that Rho-kinase activation regulates actin/myosin contractility, the expression of inflammatory mediators, and leukocyte adhesion, and transmigration across the lung endothelial cells during inflammatory responses (27). It is important to note that effects on airway smooth-muscle responses may be one of the most important factors that must be considered in the development of new therapies for asthma (5).

Several studies have reported the beneficial effects of Rho-kinase inhibition on airway hyperresponsiveness in sensitized animals (7, 9, 15, 40, 38, 43, 51). The influence of Rho-kinase on airway hyperresponsiveness appears to be, at least in part, related to agonist-mediated Ca^{2+} sensitization. The mechanisms responsible for the Ca^{2+} sensitization have not been fully elucidated, but recent studies suggest that Rho-kinase is a key protein involved in the contraction of smooth muscles; therefore, Rho-kinase presents a potential therapeutic target for asthma therapy (5, 13, 21, 37). The activated Rho-kinase promotes the phosphorylation of the myosin light chain and contributes to an increased level of muscular contraction (5, 40).

The effects of acute inhibition of Rho-kinase in sensitized animals have been analyzed in several studies (6, 11, 12, 14, 16, 37, 49, 52). Schaafsma et al. (38) showed that inhalation of Y-27632 at 30 min before and 8 h after allergen challenge in sensitized GP effectively prevents the development of airway hyperresponsiveness, after both the early and late airway reactions.

It has also been reported that Y-27632 reduces cholinergic nerve-mediated contractions in tracheal preparations of GP and mice in a dose-dependent manner (6). However, as with β_2-adrenoceptor bronchodilators, Y-27632 increases neurotransmitter release from airway cholinergic nerves. The mechanism responsible for this neurotransmitter release increase remains unclear (6, 52).

The increases in airway resistance induced by methacholine in allergic mice are also reduced with intranasal administration of Y-27632 at least 8 h after instillation of the Rho-kinase inhibitor (16). Witzenrath et al. (49) verified that the use of Y-27632 attenuated the methacholine-provoked airway response in sensitized lungs.

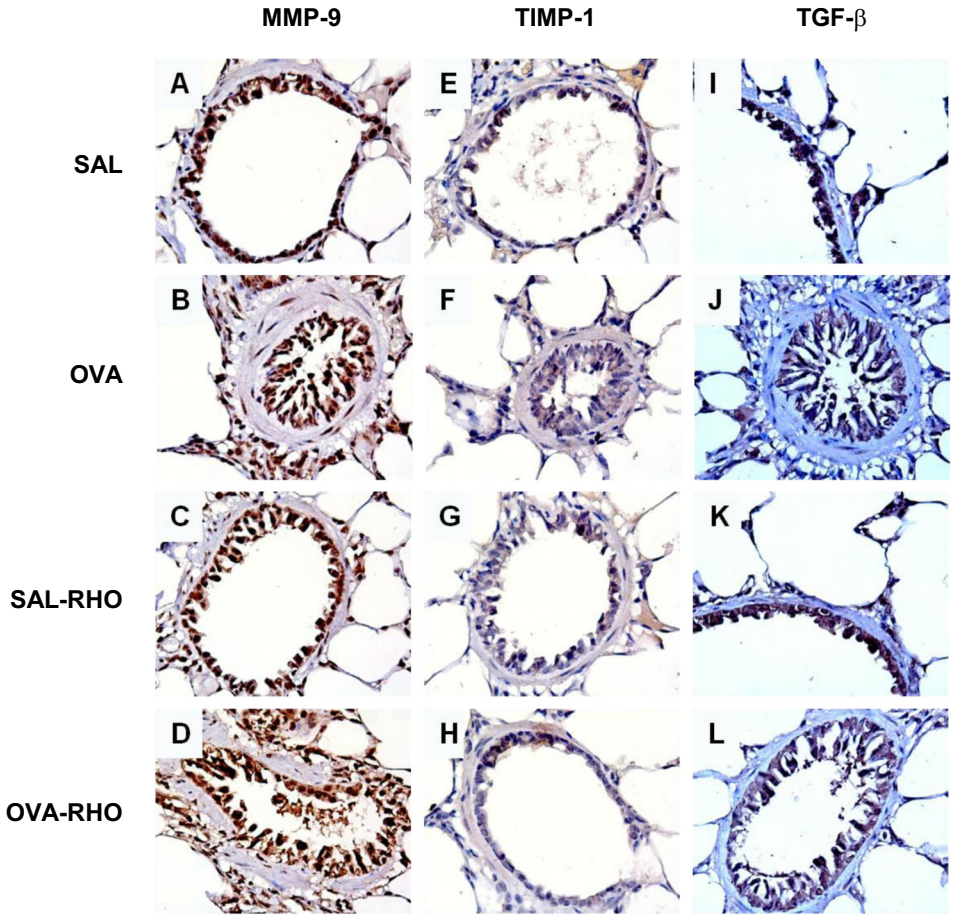

Fig. 12. Photomicrographs of the results of immunohistochemical analyses of airway walls to detect MMP-9 (*A–D*, ×400), TIMP-1 (*E–H*, ×400), and TGF-β (*I–L*, ×400). All experimental groups are represented: SAL (*A*, *E*, and *I*), OVA (*B*, *F*, and *J*), SAL-RHO (*C*, *G*, and *K*), and OVA-RHO (*D*, *H*, and *L*).

In addition to reducing airway hyperresponsiveness by promoting smooth-muscle contractility, Rho-kinase appears to mediate airway hyperresponsiveness induced by lysophosphatidic acid (14, 15). The bronchodilating action of Y-27632 was also studied as an adjuvant for isofluorane, a volatile anesthetic traditionally used to treat status asmathicus, with effects associated with both Ca^{2+}-dependent and Ca^{2+}-independent contraction in airway smooth muscles (12). Hanazaki et al. (11) reported that the isofluorane-induced relaxation of rat bronchial smooth muscle was significantly augmented by a subthreshold concentration of Y-27632.

Assuming that this may have occurred due to the acute effect of the drug on the airways, once the inhibitor Y-27632 was used 1 h before collection of data of pulmonary mechanics, we chose to create one more experimental group (OVA-wfRHO) that had not received the last inhalation. We verified that there was no difference in results of the maximal responses of *E*rs and *R*rs after ovalbumin challenge between the OVA-wfRHO and OVA-Rho groups. These data confirmed that the initial obtained results were really related to the repeated use of Y-27632 during the experimental protocol. Also, it is important to emphasize that we are not aware of any previous studies analyzing the effects of repeated Rho-kinase inhibition. We believe that repeated inhibition complements these studies in a fundamental way to demonstrate the potential importance of the Rho-kinase inhibitors in the treatment of asthma. Moreover, the experimental model used herein presents a chronic allergic inflammation response.

As in previous studies (31, 32, 44), we observed an increase in the number of eosinophils in the airways of the sensitized GP. We also noted that the Rho-kinase inhibitor significantly attenuated this response in the sensitized animals. Furthermore, we observed that Rho-kinase inhibition attenuated the numbers of IL-2-, IL-4, IL-5-, and IL-13-positive cells around the airway walls. Note that it is possible that the effects of Y-27632 on eosinophilia and cytokine expression can be partially attributed to an acute Rho-kinase inhibition, once the Rho-kinase inhibitor was used 1 h before collection of lungs for morphometric analysis. As above described, we compared the evaluation of eosinophilic infiltration in the new group OVA-wfRHO, and we did not find any differences between OVA-RHO and OVA-wfRHO animals. These results suggest that the repeated Rho-kinase inhibition modulates upstream signaling events involved in eosinophil recruitment into the airways during an allergic inflammatory response.

Several studies have suggested that the RhoA/ROCK system plays a role in eosinophil recruitment and Th-1 and Th-2 cytokine secretion (1, 2, 16). In this regard, Henry et al. (16) demonstrated that pretreatment with Y-27632 reduced the number of eosinophils recovered from the bronchoalveolar lavage (BAL) fluid of OVA-sensitized mice (16).

Taki et al. (43) demonstrated that another Rho-kinase inhibitor, fasudil, reduced the numbers of eosinophils in BAL fluid, airways, and blood vessels. This Rho-kinase inhibitor also diminished the augmented levels of IL-5, IL-13, and eotaxin in BAL fluid (43). Aihara et al. (2) showed that Y-27632 sup-

pressed the release of Th-1 cytokines and partially suppressed the release of Th-2 cytokines in healthy persons but reduced the release of IL-2 and IL-5 in asthmatic patients and weakly reduced the release of IL-4 and IFN-γ. In the present study, Rho-kinase inhibition was associated with significant reductions in levels of these interleukins and IFN-γ in animals sensitized to ovalbumin, indicating that there is indeed an association between the Rho/Rho-kinase pathway and the release of these mediators.

In this study, we also demonstrated attenuations of the number of cells positive for iNOS and the content of 8-iso-PGF2α in the area of the airway walls of sensitized animals by Rho-kinase inhibition with Y-27632. Our results are in agreement with those of McGown et al. (25), who investigated whether the Rho-kinase inhibitor fasudil protected against LPS-induced vascular leakage and leukocyte adhesion via NOS pathways. The authors demonstrated that fasudil decreased LPS-induced upregulation of iNOS, reducing microvascular inflammation.

In addition, it is well known that iNOS activation may contribute to peroxynitrite formation, which is an oxidant agent formed by the interaction of NO and superoxide. Subsequently, isoprostane generation may result from lipid peroxidation induced by peroxynitrite formation (50). The inhibition of Rho-kinase caused a reduction in the number of iNOS-positive cells, which may have contributed to the attenuation of airway hyperresponsiveness, oxidative stress, and the consequent extracellular matrix remodeling. Further studies are necessary to clarify the exact mechanisms of action of Y-27632 on NO and oxidative stress.

Regarding the assessment of changes in extracellular matrix remodeling, there was a significant decrease in the contents of collagen and elastic fibers in the group of ovalbumin-exposed animals treated with the Rho-kinase inhibitor compared with the untreated groups. There is evidence that the experimental model of chronic pulmonary inflammation is associated with increased contents of collagen and elastic fibers in the airways and distal parenchyma (3, 24, 29, 42). However, we are not aware of previous experimental studies evaluating the role of Rho-kinase inhibition on the remodeling response.

This remodeling results from repair processes in response to persistent inflammation triggered by proinflammatory mediators, metalloproteinases, cytokines, and growth factors (46). In reducing the number of inflammatory cells, Rho-kinase inhibition by Y-27632 helps to prevent chronic inflammation and indirectly contributes to a reduction of remodeling, as evidenced by the lower contents of collagen and elastic fibers in the airway walls.

It is feasible that, in addition to indirect effects on fibrosis, Rho/ROCK signaling is directly involved in profibrotic processes, mediated by airway-resident cells. Schaafsma et al. (39) showed that human airway myocytes express both geranylgeranyl transferase 1 (GGT1) and farnesyltransferase (FT), and the inhibition of GGT1, but not FT, mirrored the suppressive effects of simvastatin on collagen I and fibronectin expression and collagen I secretion. The simvastatin and GGTI-286 both prevented TGF-β1-induced membrane association of RhoA, a downstream target of GGT1, suggesting that simvastatin and GGTI-286 inhibit synthesis and secretion of extracellular matrix proteins by human airway smooth muscle cells by suppressing GGT1-mediated posttranslational modification of signaling molecules such as RhoA.

Concerning these results, there are several recent studies suggesting the importance of Rho-kinase modulation on the remodeling process. Zhou et al. (53) analyzed the effects of fasudil on high-glucose-induced proliferation of cardiac fibroblasts and collagen production. The authors demonstrated that the activation of Rho-kinase is essential for the synthesis of collagen, which may be related to a combination of factors, including the inhibition of the JNK and TGF-β pathways, which are both involved in the fibrosis process.

Kondrikov et al. (20) investigated the role of Rho-kinase and reactive oxygen species (ROS) in the synthesis of collagen type I in human and mice lung fibroblasts subjected to hyperoxia in a model of oxygen toxicity. The authors concluded that oxygen toxicity induces ROS to separate the guanine nucleotide dissociation inhibitor (a regulator of Rho GTPase activity) from Rho, which leads to activation of the Rho-kinase pathway and contributes to increased collagen-I synthesis.

It was previously reported that iNOS inhibition reduces MMP-9, TIMP-1, and TGF-β. In addition to the reduction of iNOS, we also observed attenuations of the levels of MMP-9, TIMP-1, and TGF-β in the animals treated with the Rho-kinase inhibitor. These mediators act in the production of collagen and elastic fibers, thus contributing to extracellular matrix remodeling in the airways (47). The reduced level of iNOS-positive cells in the presence of Rho-kinase inhibition found in the present study and the reduced content of collagen and elastic fibers in the treated groups are probably due to the inhibition of this pathway. The reduced numbers of iNOS-positive cells when Rho-kinase is inhibited is in agreement with the results of other studies although the underlying mechanisms are unclear (25, 41).

There appears to be a relationship between these mediators and Rho-kinase. Jiang and George (18) demonstrated that the inhibition of Rho-kinase with Y-27632 prevented the reduction of NO induction by TGF-β2, avoiding inhibition of iNOS, suggesting that TGF-β2 inhibits iNOS expression via the Rho-kinase pathway in lung epithelial cells.

We also found that the level of another important inflammatory mediator, NF-κB, was reduced in the sensitized animals treated with the Rho-kinase inhibitor compared with the untreated animals. Similarly, Meyer-Schwezinger et al. (26), when evaluating the role of Rho-kinase in inflammatory renal injury in mice, found that the inhibition of Rho-kinase was related to an attenuation of NF-κB signaling, resulting in protection against injury. These data suggest that the NF-κB signaling is also Rho-kinase dependent. The presence of airway smooth muscle tissue hypertrophy reinforces the idea that we used a model of chronic pulmonary inflammation and that the repeated use of Y-27632 attenuated this response.

The present study has several limitations. We used Rho-kinase inhibition by Y-27632 in an experimental model of chronic airway inflammation. We advise caution when extrapolating our findings directly to human physiology. However, our results support the importance of Rho-kinase in airway hyperresponsiveness, lung inflammatory responses, extracellular matrix remodeling, and oxidative stress pathway.

Additionally, it is important to note that the GP model is one of the best animal models for the study of asthma due to the similar lung anatomy of humans and GP and the presence of

several characteristics of human asthma such as eosinophilic inflammatory and remodeling process (34). Additional studies are needed to elucidate the exact mechanisms responsible for these changes.

In conclusion, Rho-kinase pathway activation modulates hyperresponsiveness, inflammation, the extracellular matrix remodeling process, and oxidative stress activation. These results suggest that Rho-kinase inhibitors constitute potential pharmacological tools for the control of asthma.

ACKNOWLEDGMENTS

We thank Sandra de Moraes Fernezlian and Esmeralda Meristene for skillful technical assistance. We also thank Maria Luiza Vilela Oliva for execution of several of the experiments.

GRANTS

This work was suppored by the Fundação de Amparo à Pesquisa do Estado de São Paulo (FAPESP).

DISCLOSURES

No conflicts of interest, financial or otherwise, are declared by the authors.

AUTHOR CONTRIBUTIONS

Author contributions: S.S.P., E.A.L.-M., M.A.M., and I.d.F.L.C.T. conception and design of research; S.S.P., H.T.C., R.F.R., P.A.d.S., R.A.-R., B.M.S.-R., A.P., and C.M.P. performed experiments; S.S.P. and H.T.C. analyzed data; S.S.P. and I.d.F.L.C.T. interpreted results of experiments; S.S.P. prepared figures; S.S.P. and I.d.F.L.C.T. drafted manuscript; S.S.P. and I.d.F.L.C.T. edited and revised manuscript; S.S.P. and I.d.F.L.C.T. approved final version of manuscript.

REFERENCES

1. **Aihara M, Dobashi K, Iizuka K, Nakazawa T, Mori M.** Comparison of effects of Y-27632 and Isoprotenerol on release of cytolines from human peripheral T cells. *Int Immunopharmacol* 3: 1619–1625, 2003.
2. **Aihara M, Dobashi K, Iizuka K, Nakazawa T, Mori M.** Effect of Y-27632 on release of cytokines from peripheral T cells in asthmatic patients and normal subjects. *Int Immunopharmacol* 4: 557–561, 2004.
3. **Angeli P, Prado CM, Xisto DG, Silva PL, Pássaro CP, Nakazato HD, Leick-Maldonado EA, Martins MA, Rocco PR, Tibério IF.** Effects of chronic L-NAME treatment lung tissue responses induced by chronic pulmonary inflammation mechanics, eosinophilic and extracellular matrix. *Am J Physiol Lung Cell Mol Physiol* 294: L1197–L1205, 2008.
4. **Bukstein D, Luskin AT, Brooks EA.** Exhaled nitric oxide as a tool in managing and monitoring difficult-to-treat asthma. *Allergy Asthma Proc* 32: 1–8, 2011.
5. **Chiba Y, Matsusue K, Misawa M.** RhoA, a possible target for treatment of airway hyperresponsiveness in bronchial asthma. *J Pharm Sci* 114: 239–247, 2010.
6. **Fernandes L, D'Aprile A, Self G, McGuire M, Sew T, Henry P, Goldie R.** A Rho-kinase inhibitor, Y-27632, reduces cholinergic contraction but not neurotransmitter release. *Eur J Pharmacol* 550: 155–161, 2006.
7. **Girodet PO, Ozier A, Bara I, Lara JMT, Marthan R, Berger P.** Airway remodeling in asthma: new mechanisms and potential for pharmacological intervention. *Pharmacol Ther* 130: 325–337, 2011.
8. **Global Initiative for Asthma (GINA).** *Global Strategy for Asthma Management and Prevention.* http://www.ginasthma.org/ [2011].
9. **Gosens R, Schaafsma D, Bromhaar MMG, Vrugt B, Zaagsma J, Meurs H, Nelemans SA.** Growth factor-induced contraction of human bronchial smooth muscle is Rho-kinase-dependent. *Eur J Pharmacol* 494: 73–76, 2004.
10. **Gundersen HJ, Bagger P, Bendtsen TF, Evans SM, Korbo L, Marcussen N, Moller A, Nielsen K, Nyengaard JR, Pakkenberg B, Sorensen FB, Vesterby A, West MJ.** The new stereological tools: disector, fractionator, nucleator and point sampled intercepts and their use in pathological research and diagnosis. *APMIS* 96: 857–881, 1988.
11. **Hanazaki M, Chiba Y, Yokoyama M, Morita K, Kohjitani A, Sakai H, Misawa M.** Y-27632 augments the isoflurane-induced relaxation of bronchial smooth muscle in rats. *J Smooth Muscle Res* 44: 189–193, 2008.
12. **Hanazaki M, Jones KA, Warner DO.** Effects of intravenous anesthetics on Ca^{2+} sensitivity in canine tracheal smooth muscle. *Anesthesiology* 92: 133–139, 2000.
13. **Hashimoto K, Peebles RS Jr, Sheller JR, Jarzecka K, Furlong J, Mitchell DB, Hartert TV, Graham BS.** Suppression of airway hyperresponsiveness induced by ovalbumin sensitization and RSV infection with Y-27632, a Rho kinase inhibitor. *Thorax* 57: 524–527, 2002.
14. **Hashimoto T, Nakano Y, Ohata H, Momose K.** Lysophosphatidic acid enhances airway response to acetylcholine in guinea pigs. *Life Sci* 70: 199–205, 2001.
15. **Hashimoto T, Nakano Y, Yamashita M, Fang Y, Ohata H, Momose K.** Role of Rho-associated protein kinase and histamine in lysophosphatidic acid induced airway hyperresponsiveness in guinea pigs. *Jpn J Pharmacol* 88: 256–261, 2002.
16. **Henry PJ, Mann TS, Goldie RG.** A Rho kinase inhibitor, Y-27632 inhibits pulmonary eosinophilia, bronchoconstriction and airways hyperresponsiveness in allergic mice. *Pulm Pharmacol Ther* 18: 67–74, 2005.
17. **Iizuka K, Shimizy Y, Tsukagoshi H, Yoshii A, Harada T, Dobashi K, Murozono T, Nakazawa T, MoriM.** Evaluation of Y-27632, a Rho-kinase inhibitor, as a bronchodilator in guinea pigs. *Eur J Pharmacol* 406: 273–279, 2000.
18. **Jiang J, George SC.** TGF-β_2 reduces nitric oxide synthase mRNA through a ROCK-dependent pathway in airway epithelial cells. *Am J Physiol Lung Cell Mol Physiol* 301: L361–L367, 2011.
19. **Kharitonov AS, Yates DH, Robbins RA, Logan-Sinclair R, Shinebourne EA, Barnes PJ.** Increases nitric oxide in exhaled air of asthmatic patients. *Lancet* 343: 133–135, 1994.
20. **Kondrikov D, Caldwell RB, Dong Z, Su Y.** Reactive oxygen species-dependent RhoA activation mediates collagen synthesis in hyperoxic lung fibrosis. *J Pharmacol Exper Ther* 337: 628–635, 2011.
21. **Kureishi Y, Kobayashi S, Amano M, Kimura K, Kanaide H, Nakano T, Kaibuchi K, Ito M.** Rho-associated kinase directly induces smooth muscle contraction through myosin light chain phosphorylation. *J Biol Chem* 272: 12257–12260, 1977.
22. **Lanças T, Kasahara DI, Prado CM, Tibério IFLC, Martins MA, Dolhnikoff M.** Comparison of early and late responses to antigen of sensitized guinea pig parenchymal lung strips. *J Appl Physiol* 100: 1610–1616, 2006.
23. **Leick-Maldonado EA, Kay FU, Leonhardt MC, Kasahara DI, Prado CM, Fernandes FT, Martins MA, Tibério IFLC.** Comparison of glucocorticoid and cysteinyl leukotriene receptor antagonist treatments in an experimental model of chronic airway inflammation in guinea-pigs. *Clin Exp Allergy* 34: 145–152, 2004.
24. **Mauad T, Silva LF, Santos MA, Grinberg L, Bernardi FD, Martins MA, Saldiva PH, Dolhnikoff M.** Abnormal alveolar attachments with decreased elastic fiber content in distal lung in fatal asthma. *Am J Respir Crit Care Med* 170: 857–862, 2004.
25. **McGown CM, Brown NJ, Hellewell PG, Brookes ZLS.** ROCK induced inflammation of the microcirculation during endotoxemia mediated by nitric oxide synthase. *Microvasc Res* 81: 281–288, 2011.
26. **Meyer-Schwesinger C, Dehde S, von Ruffer C, Gatzmeier S, Klug P, Wenzel UO, Stahl RA, Thaiss F, Meyer TN.** Rho kinase inhibition attenuates LPS-induced renal failure in mice in part by attenuation of NF-κB p65 signaling. *Am J Physiol Renal Physiol* 296: F1088–F1099, 2009.
27. **Mong PY, Wang Q.** Activation of Rho kinase isoforms in lung endothelial cells during inflammation. *J Immunol* 182: 2385–2394, 2009.
28. **Mota I, Perini A.** A heat labile mercaptoethanol susceptible homocytotropic antibody in the guinea pig. *Life Sci II* 9: 923–930, 1970.
29. **Nakashima AS, Prado CM, Lancas T, Ruiz VC, Kasahara DI, Leick-Maldonado EA, Dolhnikoff M, Martins MA, Tibério IF.** Oral tolerance attenuates changes in in vitro lung tissue mechanics and extracellular matrix remodeling induced by chronic allergic inflammation in Guinea pigs. *J Appl Physiol* 104: 1778–1785, 2008.
30. **Prado CM, Leick-Maldonado EA, Arata V, Kasahara DI, Martins MA, Tibério IFLC.** Neurokinins and inflammatory cell iNOS expression in guinea pigs with chronic allergic airway inflammation. *Am J Physiol Lung Cell Mol Physiol* 288: L741–L748, 2005.
31. **Prado CM, Leick-Maldonado EA, Kasahara DI, Capelozzi VL, Martins MA, Tibério IFLC.** Effects of acute and chronic nitric oxide inhibition in an experimental model of chronic pulmonary allergic inflammation in guinea pigs. *Am J Physiol Lung Cell Mol Physiol* 289: L677–L683, 2005.

32. **Prado CM, Leick-Maldonado EA, Yano L, Leme AS, Capelozzi VL, Martins MA, Tiberio IF.** Effects of nitric oxide synthases in chronic allergic airway inflammation and remodeling. *Am J Respir Cell Mol Biol* 35: 457–465, 2006.
33. **Prado CM, Yano L, Rocha G, Starling CM, Capelozzi VL, Leick-Maldonado EA, Martins MA, Tibério IF.** Effects of nitric oxide synthase inhibition in bronchial vascular remodeling-induced by chronic allergic pulmonary inflammation. *Exp Lung Res* 37: 259–268, 2011.
34. **Ricciardolo FLM, Sterk PJ, Gaston B, Folkerts G.** Nitric oxide in health and disease of the respiratory system. *Physiol Rev* 84: 731–765, 2004.
35. **Ruiz-Schütz VC, Drewiacki T, Nakashima AS, Arantes-Costa FM, Prado CM, Kasahara DI, Leick-Maldonado EA, Martins MA, Tibério IF.** Oral tolerance attenuates airway inflammation and remodeling in a model of chronic pulmonary allergic inflammation. *Respir Physiol Neurobiol* 165: 13–21, 2009.
36. **Sakae RS, Leme AS, Dolhnikoff M, Pereira PM, do Patrocinio M, Warth TN, Zin WA, Saldiva PH, Martins MA.** Neonatal capsaicin treatment decreases airway and pulmonary tissue responsiveness to methacholine. *Am J Physiol Lung Cell Mol Physiol* 266: L23–L29, 1994.
37. **Schaafsma D, Bos ST, Zuidhof AB, Zaagsma J, Meurs H.** Inhalation of the Rho-kinase inhibitor Y-27632 reverses allergen-induced airway hyperresponsiveness after the early and late asthmatic reaction. *Respir Res* 7: 121, 2006.
38. **Schaafsma D, Bos ST, Zuidhof AB, Zaagsma J, Meurs H.** The inhaled Rho kinase inhibitor Y-27632 protects against allergen-induced acute bronchoconstriction, airway hyperresponsiveness, and inflammation. *Am J Physiol Lung Cell Mol Physiol* 295: L214–L219, 2008.
39. **Schaafsma D, Dueck G, Ghavami S, Kroeker A, Mutawe MM, Hauff K, Xu FY, McNeill KD, Unruh H, Hatch GM, Halayko AJ.** The mevalonate cascade as a target to suppress extracellular matrix synthesis by human airway smooth muscle. *Am J Respir Cell Mol Biol* 44: 394–403, 2011.
40. **Schaafsma D, Gosens R, Bos ST, Meurs H, Zaagsma J, Nelemans A.** Allergic sensitization enhances the contribution of Rho-kinase to airway smooth muscle contraction. *Br J Pharmacol* 143: 477–484, 2004.
41. **Soliman H, Craig GP, Nagareddy P, Yuen VG, Lin G, Kumar U, McNeill JH, Macleod KM.** Role of inducible nitric oxide synthase in induction of RhoA expression in hearts from diabetic rats. *Cardiovasc Res* 79: 322–330, 2008.
42. **Starling CM, Prado CM, Leick-Maldonado EA, Lanças T, Reis FG, Aristóteles LR, Dolhnikoff M, Martins MA, Tibério IF.** Inducible nitric oxide synthase inhibition attenuates lung tissue responsiveness and remodeling in a model of chronic pulmonary inflammation in guinea pigs. *Respir Physiol Neurobiol* 165: 185–194, 2009.
43. **Taki F, Kume H, Kobayashi T, Ohta H, Aratake H, Shimokata K.** Effects of Rho-kinase inactivation on eosinophilia and hyperreactivity in murine airways by allergen challenges. *Clin Exp Allergy* 37: 599–607, 2007.
44. **Tibério IF, Turco GM, Leick-Maldonado EA, Sakae RS, Paiva SO, do Patrocinio M, Warth TN, Lapa e Silva JR, Saldiva PH, Martins MA.** Effects of neurokinin depletion on airway inflammation induced by chronic antigen exposure. *Am J Respir Crit Care Med* 155: 1739–174, 1997.
45. **Uehata M, Ishizaki T, Satoh H, Ono T, Kawahara T, Morishita T, Tamakawa H, Yamagami K, Inui J, Maekawa M, Narumiya S.** Calcium sensitization of smooth muscle mediated by a Rho-associated protein kinase in hypertension. *Nature* 389: 990–994, 1997.
46. **Vignola AM, Kips J, Bousquet J.** Tissue remodeling as a feature of persistent asthma. *J Allergy Clin Immunol* 105: 1041–1053, 2000.
47. **Vignola AM, Mirabella F, Costanzo G, Di Giorgi R, Gjomarkaj M, Bellia V, Bonsignore G.** Airway remodeling in asthma. *Chest* 123: 417S–422S, 2003.
48. **Watanabe T, Okano M, Hattori H, Yoshino T, Ohno N, Ohta N, Sugata Y, Orita Y, Takai T, Nishizaki K.** Roles of FcgammaRIIB in nasal eosinophilia and IgE production in murine allergic rhinitis. *Am J Respir Crit Care Med* 169: 105–112, 2004.
49. **Witzenrath M, Ahrens B, Schmeck B, Kube SM, Hippenstiel S, Rosseau S, Hammelmann E, Suttorp N, Schütte H.** Rho-kinase and contractile apparatus proteins in murine airway hyperresponsiveness. *Exp Toxicol Pathol* 60: 9–15, 2008.
50. **Xia Y, Tsai AL, Berka V, Zweier JL.** Superoxide generation from endothelial nitric-oxide synthase. A Ca2+/calmodulin-dependent and tetrahydrobiopterin regulatory process. *J Biol Chem* 273: 25804–25808, 1998.
51. **Yoshii A, Iizuka K, Dobashi K, Horie T, Harada T, Nakazawa T, Mori M.** Relaxation of contracted rabbit tracheal and human bronchial smooth muscle by Y-27632 through inhibition of Ca^{2+} sensitization. *Am J Respir Cell Mol Biol* 20: 1190–1200, 1999.
52. **Zhang XY, Olszewski MA, Robinson NE.** β_2-adrenoceptor activation augments acetylcholine release from tracheal parasympathetic nerves. *Am J Physiol* 12: 950–956, 1995.
53. **Zhou H, Zhang KX, Li YJ, Guo BY, Wang M, Wang M.** Fasudil hydrochloride hydrate, a Rho-kinase inhibitor, suppresses high glucose-induced proliferation and collagen synthesis in rat cardiac fibroblasts. *Clin Exp Pharmacol Physiol* 38: 387–394, 2011.